Donor bound excitons involving a hole from the B valence band in ZnO: Time resolved and magneto-photoluminescence studies

Shula Chen, Weimin Chen and Irina Buyanova

Original Publication:

Shula Chen, Weimin Chen and Irina Buyanova, Donor bound excitons involving a hole from the B valence band in ZnO: Time resolved and magneto-photoluminescence studies, 2011, Applied Physics Letters, (99), 9, 091909.
http://dx.doi.org/10.1063/1.3628332

Donor bound excitons involving a hole from the B valence band in ZnO: Time resolved and magneto-photoluminescence studies

S. L. Chen, W. M. Chen, and I. A. Buyanova[a)]
Department of Physics, Chemistry and Biology, Linköping Univeristy, 58183 Linköping, Sweden

(Received 27 May 2011; accepted 3 August 2011; published online 1 September 2011)

Time-resolved and magneto-photoluminescence (PL) studies are performed for the so-called I_6^B and I_7^B excitonic transitions, previously attributed to neutral donor bound excitons involving a hole from the B valence band (VB), D^0X^B. It is shown that PL decays of these emissions at 2 K are faster than that of their I_6 and I_7 counterparts involving an A VB hole, which is interpreted as being due to energy relaxation of the hole assisted by acoustic phonons. From the magneto-PL measurements, values of effective Landé g factors for conduction electrons and B VB holes are determined as $g_e = 1.91$, $g_h^{//} = 1.79$, and $g_h^{\perp} = 0$, respectively. © *2011 American Institute of Physics*. [doi:10.1063/1.3628332]

ZnO is a direct and wide bandgap semiconductor which continues to attract enormous attention as a promising material for a wide variety of applications, e.g., in highly efficient optoelectronic devices.[1] In spite of high interest and extensive research efforts, however, many fundamental properties of this material are not yet fully understood. For example, it is well known that the crystal field and spin-orbit interactions cause splitting of valence band (VB) states in ZnO into the so-called A, B, and C subbands. However, there has been a long-standing debate on the exact symmetry of these states, i.e., Γ_7, Γ_9, Γ_7 vs Γ_9, Γ_7, Γ_7.[2–10] Only until most recently, the former ordering of the VB states became favored, based on first-principle band structure calculations[8] and detailed magneto-optical studies[10–12] of the donor bound excitons involving an A-VB hole (DX^A). These studies have also provided consistent information regarding the sign and value of the Landé g factor for the Γ_7-hole. As to the properties of the B-VB subband, data available so far are rather scarce.[8,13] The knowledge of these properties is important for successful applications of ZnO, as the population of the B-VB state rapidly increases with rising temperature because of the small A-B energy splitting of 4.5 meV and becomes substantial at temperatures relevant to device operation.

Similar to the A-VB state, the B-VB state could be studied via related optical transitions, such as transitions involving excited states of donor bound excitons where an A-VB hole is replaced by a hole from the B-VB (the so-called DX^B). This is shown schematically in Fig. 1(a), taking as an example, excitons bound to a neutral donor (D^0X). In such D^0X states, two electrons of the Γ_7 symmetry are paired with anti parallel spins, whereas the participating hole is $A(\Gamma_7)$ for the lower D^0X^A state and $B(\Gamma_9)$ for the higher lying D^0X^B level. The energy separation between D^0X^A and D^0X^B is determined by the A-B splitting.[7,14,15] It was recently suggested[15] that the D^0X^B, though weak, can be detected in low-temperature photoluminescence (PL) spectra in high quality ZnO, in addition to intense emissions from D^0X^A. The purpose of this work is to understand dynamics and magneto-optical properties of the D^0X^B excitons by using magneto-PL and transient PL spectroscopies.

Several undoped wurzite ZnO substrates were studied. PL measurements were carried at temperatures of 2-25 K in a magnetic field up to 10 T. Continuous-wave (cw) PL was excited by the 266 nm line of a solid state laser and was detected by a photomultiplier assembled with a 0.8-m monochromator. Time-resolved PL measurements were performed using a tunable Ti: sapphire pulsed laser with an excitation wavelength of 266 nm, a repetition rate of 76 MHz, and a pulse duration of ~150 fs. Transient PL was detected by a streak camera combined with a 0.5 m monochromator.

Typical PL spectra measured at 9 and 15 K are shown in Fig. 2(a) and are governed by excitonic emissions involving A-VB holes. These include the D^0X^A transitions of I_9, I_7, and I_6,[14] excitons bound to ionized donors D^+X^A (the I_0 line) and free A-exciton (FX^A) emissions from the upper (FX^A_u) and lower (FX^A_l) polariton branches. In addition, the spectra contain emission lines denoted as I_6^B and I_7^B in Fig. 2, which are separated by 4.4-4.5 meV from I_6 and I_7 respectively. Both I_6^B and I_7^B have previously been assigned[15] to the excited states of the I_6 and I_7 excitons involving a B-VB hole see Fig. 1(a). Intensity of these

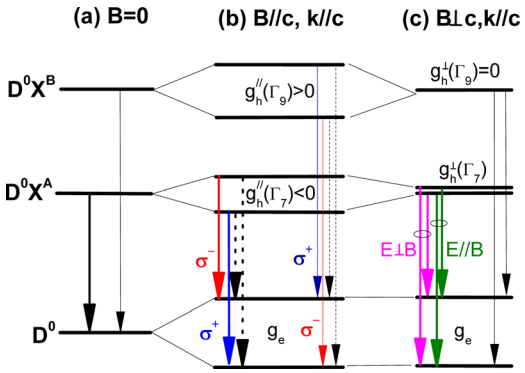

FIG. 1. (Color online) Schematic energy diagrams of a neutral donor bound exciton at B = 0 (a), in the Faraday (b), and in the Voigt (c) geometries. In (a), the thick and thin arrows denote the exciton transitions involving a hole from the $A(\Gamma_7)$ and $B(\Gamma_9)$ VB subbands, respectively. The solid (dashed) arrows in (b) represent the transitions that can (cannot) be observed in the given geometry.

a)Author to whom correspondence should be addressed. Electronic mail: iribu@ifm.liu.se.

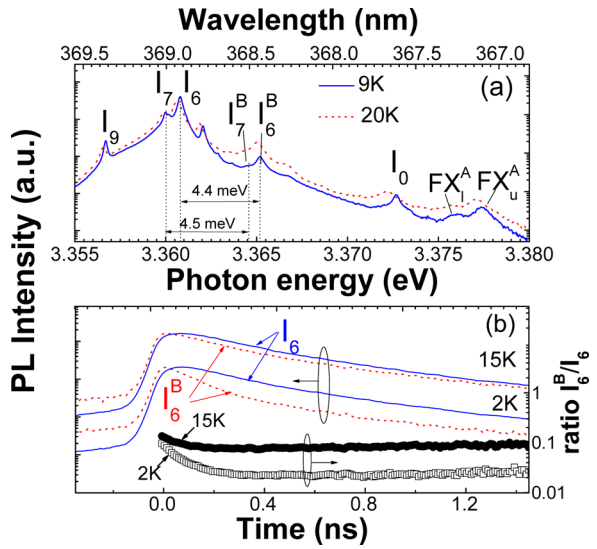

FIG. 2. (Color online) (a) Typical PL spectra of undoped bulk ZnO displayed in the logarithmic scale. A shift between the PL maxima positions at 9 K and 15 K is due to a thermal variation of the bandgap energy. (b) PL decays measured at 2 K and 15 K for I_6 (solid lines) and I_6^B (dotted lines) displayed in the logarithmic scale. The decays are normalized to the same peak intensity. The decays at 2 K and 15 K are offset vertically, for clarity. Also shown is temporal evolution of the I_6^B/I_6 ratio measured at 2 K (solid circles) and 15 K (open squares).

emissions is found to increase with increasing temperature, reflecting increasing population of the B-VB holes. Moreover, the linewidths of I_6^B and I_7^B are significantly broader than that of I_6 and I_7. For example, whereas the full-width-at-half-maximum of I_6 is 0.4 meV at 9 K, it is around 1 meV for I_6^B. In principle, such broadening may occur for excited states of bound excitons due to lifetime broadening[16] caused by fast energy relaxation down to their ground states.

To understand dynamics of I_6^B and I_7^B, we performed time-resolved PL measurements. Both transitions were found to exhibit very similar transient and magneto-optical properties indicative for their similar origin. Therefore, in the following discussion, we will concentrate on the I_6-related emissions. Representative PL decays and temporal evolution of the I_6^B/I_6 ratio measured at 2 K and 15 K are shown in Fig. 2(b). Both rising time and initial decay of I_6^B at 2 K are found to be substantially shorter than that for I_6, whereas both emissions decay with a similar rate at a longer time (>0.4 ns) after the excitation pulse. Their PL transients become very similar at $T \geq 15$ K. The observed transient behavior is in principle consistent with the origin of I_6^B as being from the excited state D^0X^B suggested in Ref. 15. Indeed, the observed slower rising of I_6 indicates involvement of feeding processes, e.g., from the D^0X^B state, that are known to be efficient from PL excitation measurements.[7,14] The initial fast decay of I_6^B at 2 K can then be interpreted as being related to the energy relaxation to the D^0X^A state, which shortens the lifetime of the D^0X^B. This process should be assisted by acoustic phonons since the energy splitting between the two exciton states is much smaller than the optical phonon energy of 72 meV. A characteristic time of ~100-200 ps estimated for such relaxation process from our transient PL data is of the same order as the inter-VB hole relaxation time reported for CdSe and CdS.[17] After the thermalization process is completed, both states are expected to decay at a similar rate determined by their recombination time, as indeed observed experimentally. We note, however, several observations that do not necessarily imply the aforementioned scenario. First of all, under the above bandgap excitation employed here, trapping to the D^0X^A state does not primarily occur from the excited state D^0X^B as the rising time of I_6 is shorter than the fast component of the I_6^B decay. Moreover, one would expect that the energy relaxation between the B and A VB states should drive their populations towards the Boltzmann distribution, provided that the energy relaxation time is much shorter than the exciton recombination time. This is indeed observed at 15 K, where the I_6^B/I_6 ratio saturates with time at 0.07, i.e., close to the value of 0.034 expected in thermal equilibrium—see Fig. 2(b). At 2K, however, the measured saturation value is around 0.02 which by far exceeds the thermal equilibrium value. Under the assumption that the I_6^B emission indeed originates from the D^0X^B state, this could be tentatively attributed to scattering/up-conversion processes which enhance the D^0X^B population. Though the exact origin of these processes is currently unclear, it is interesting to note that a similarly high population of the B-VB state was also observed in the transient PL spectra of CdSe and CdS.[17]

Let us now discuss magneto-optical properties of I_6^B and I_6. The expected effects of an applied magnetic field $\boldsymbol{B}$ on the optical transitions of D^0X are illustrated schematically in Figs. 1(b) and 1(c). A magnetic field lifts degeneracy of the donor ground state D^0 and exciton states D^0X, of which each will split into two components with their energy separations determined by the electron and hole g-factors, respectively. The electron g-factor g_e is nearly isotropic whereas the effective hole g-factor g_h is highly anisotropic and can be defined as $g_h = \sqrt{\left(g_h^{//}\cos(\theta)\right)^2 + \left(g_h^{\perp}\cos(\theta)\right)^2}$.[17] Here, $g_h^{//}$ and $g_h^{\perp}$ denote components parallel and perpendicular to the c-axis, and θ is the angle between the c-axis and $\boldsymbol{B}$. $g_h^{\perp} \neq 0$ but is low (0.02-0.25) for the Γ_7 hole,[10–12] whereas $g_h^{\perp}(\Gamma_9) = 0$ from group symmetry considerations.[16] Therefore, though splitting of the excitonic transitions in the Voigt configuration ($\boldsymbol{B} \perp c$, $c \| k$) is mainly determined by the Zeeman splitting of D^0, extra components due to non-zero $g_h^{\perp}(\Gamma_7)$ are expected for D^0X^A that can be resolved in linear polarizations (Fig. 1(c)). This prediction was recently confirmed for the I_6^* and I_4 lines,[11] which unambiguously proved the Γ_7 character of the involved hole. In the Faraday geometry ($\boldsymbol{B} \| c$, $c \| k$), two circularly polarized optical transitions can be observed for D^0X^A and D^0X^B with the corresponding Zeeman splittings of $[g_e + g_h^{//}(\Gamma_7)]\mu_B B$ and $[g_e - g_h^{//}(\Gamma_9)]\mu_B B$, respectively. Here μ_B denotes the Bohr magneton. These transitions are shown by the solid lines and are labeled as σ^+ and σ^- in Fig. 1(b). The other two transitions (dotted lines in Fig. 1(b)) cannot be observed in the Faraday configuration but can become visible when $\boldsymbol{B}$ is not parallel to c.

Magneto-PL spectra from the investigated ZnO samples are shown in Fig. 3. For clarity, only spectral ranges corresponding to the I_6 and I_6^B lines are shown. The field induced splitting of I_6 can be fully understood assuming that $|g_h^{\|}(\Gamma_7)| < g_e$ and is negative. The observation of four PL lines in the Voigt configuration by separately detecting

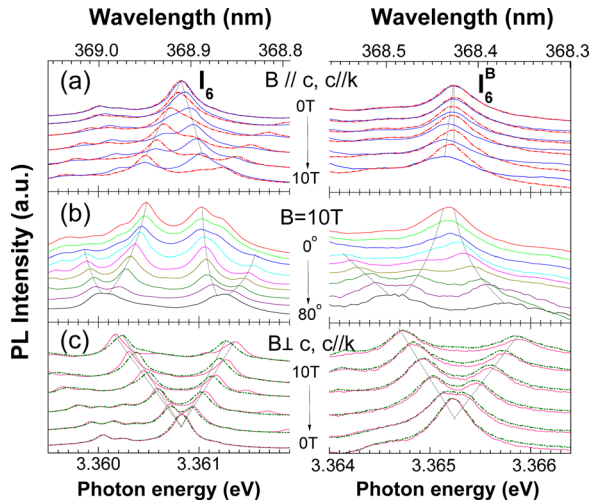

FIG. 3. (Color online) Magneto-PL spectra measured at 9K within the spectral ranges of the I_6 and I_6^B emissions. The spectra detected in σ^- and σ^+ polarizations are show in (a) by the dotted and solid lines, respectively. The solid (dotted) curves in (c) denote spectra measured under linearly polarized detection with $\mathbf{E}\perp\mathbf{B}$ ($\mathbf{E}//\mathbf{B}$). The spectra are offset vertically, for clarity.

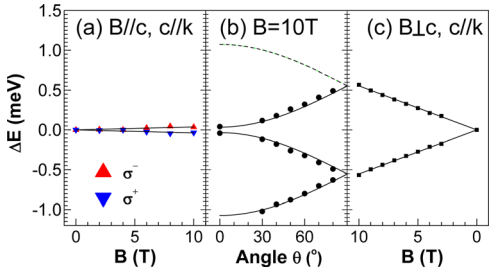

FIG. 4. (Color online) Zeeman splitting of the I_6^B line as a function of B in the Faraday (a) and Voigt (c) geometries. (b) Angular dependence of the Zeeman components measured at 10 T. The symbols denote experimental data, whereas the lines are simulation results. In the Faraday geometry, peak positions of the PL emission were detected in the σ^- and σ^+ polarizations. All energies are plotted with respect to the center-of-gravity of the Zeeman components.

linearly polarized PL in two cross polarizations (Fig. 3(c)) unambiguously proves that I_6 involves a Γ_7 hole. By fitting the fan diagram and angular dependences of the observed Zeeman splitting, the electron and effective hole g factors can be deduced as $g_e = 1.92$, $g_h^{//}(\Gamma_7) = 1.04$, and $g_h^{\perp}(\Gamma_7) = 0.2$, consistent with the values reported in Refs. 8, 10, and 12.

As to the I_6^B line, only a small splitting was observed in the Faraday geometry by detecting σ^- and σ^+ polarizations (see Fig. 3(a)). The splitting becomes apparent with increasing angle θ (see Fig. 3(b)). For $\theta > 30°$, one also notices an extra low energy PL component that gradually shifts to higher energies with increasing θ. In the Voigt configuration, only two Zeeman components are observed for I_6^B, in sharp contrast to I_6—see Fig. 3(c). The energy positions of all observed components of I_6^B as a function of B and θ are plotted in Fig. 4.

The observed field and angular dependences of I_6^B (I_7^B) are consistent with its assignment to D^0X^B. Indeed, the splitting of only two components in the Voigt configuration testifies that $g_h^{\perp} = 0$, i.e., the involved hole could belong to the Γ_9 VB state (see Fig. 1(c)). The observed σ^- polarization and higher intensity of the high energy component of I_6^B in the Faraday configuration implies that this transition concerns the lower Zeeman-split level of D^0X^B, which in turn means that $g_h^{//} < g_e$ and $g_h^{//} > 0$. Under these assumptions, excellent agreement between the experimental data and the simulations (shown by the solid lines in Fig. 4) is achieved. The lack of the uppermost branch (shown by the dotted line in Fig. 4) could be attributed to the low population of the upper Zeeman-split level of D^0X^B. The best fit is obtained assuming that $g_e = 1.91$, $g_h^{//}(\Gamma_9) = 1.79$, and $g_h^{\perp}(\Gamma_9) = 0$. The derived value of the electron g factor is in good agreement with that deduced for I_6 and also with the previously reported values.[10–12] On the other hand, the value of $g_h^{//}$ is lower than the theoretically predicted value of $g_h^{//}(\Gamma_9) \sim 3$ (Ref. 8) for a Γ_9 hole participating in the D^0X^B but is close to the value of 1.95 previously reported for the B-VB hole from reflection measurements.[7] Our results, therefore, call for further theoretical studies of the B excitons in an applied magnetic field.

In conclusion, we have performed comprehensive time-resolved and magneto-PL studies of the I_6^B and I_7^B excitonic transitions previously attributed to neutral donor bound excitons involving a hole from the B VB. We show that the PL decays of these emissions are faster than those measured for the I_6 and I_7 transitions, which could be attributed to the intra VB energy relaxation assisted by acoustic phonons. The observed splitting of the I_6^B and I_7^B lines in an applied magnetic field suggests that these emissions originate from the D^0X excitons with $g_e = 1.91$, $g_h^{//} = 1.79$, and $g_h^{\perp} = 0$.

Financial support by the Swedish Research Council (Grant No. 621-2010-3971) is greatly appreciated.

[1]For a recent review, see e.g., C. Klingshirn, Phys. Status Solidi B **244**, 3027 (2007).
[2]D. C. Reynolds, C. W. Linton, and T. C. Collins, Phys. Rev. A **140**, 1726 (1965).
[3]D. G. Thomas, J. Phys. Chem. Solids **15**, 86 (1960).
[4]D. C. Reynolds, D. C. Look, and B. Jogai, C. W. Linton, G. Cantwell, and W. C. Harsch, Phys. Rev. B **60**, 2340 (1999).
[5]K. Hummer, Phys. Status Solidi B **86**, 527 (1978).
[6]P. Loose, M. Rosenzweig, and M. Wohleche, Phys. Status Solidi B **75**, 137 (1976).
[7]G. Blattner, C. Klingshirn, R. Helbig, and R. Meinl, Phys. Status Solidi B **107**, 105 (1981).
[8]W. R. L. Lambrecht, A. V. Rodina, S. Limpijumnong, B. Segall, and B. K. Meyer, Phys. Rev. B **65**, 075207 (2002).
[9]S. F. Chichibu, T. Sota, G. Cantwell, D. B. Eason, and C. W. Litton, J. Appl. Phys. **93**, 756 (2003).
[10]A. V. Rodina, M. Strassburg, M. Dworzak, U. Haboeck, A. Hoffmann, A. Zeuner, H. R. Alves, D. M. Hofmann, and B. K. Meyer, Phys. Rev. B **61**, 125206 (2004).
[11]M. R. Wagner, J. H. Schulze, R. Kirste, M. Cobet, A. Hoffmann, C. Rauch, A. V. Rodina, B. K. Meyer, U. Röder, and K. Thonke, Phys. Rev. B **80**, 205203 (2009).
[12]L. Ding, B. K. Li, H. T. He, W. K. Ge, J. N. Wang, J. Q. Ning, X. M. Dai, C. C. Ling, and S. J. Xu, J. Appl. Phys. **105**, 053511 (2009).
[13]G. Blattner, G. Kurtze, G. Schmieder, and C. Klingshirn, Phys. Rev. B **255**, 7413 (1982).
[14]J. Gutowski, N. Presser, and I. Broser, Phys. Rev. B **38**, 9724 (1988).
[15]B. K. Meyer, J. Sann, S. Eisermann, S. Lautenschlaeger, M. R. Wagner, M. Kaiser, G. Callsen, J. S. Reparaz, and A. Hoffmann, Phys. Rev. B **82**, 115207 (2010).
[16]D. G. Thomas and J. J. Hopfield, Phys. Rev. **128**, 2135 (1962).
[17]H. Yoshida, H. Saito, and S. Shionoya, J. Phys. Soc. Jpn. **50**, 881 (1981).